IEEE Access
Multidisciplinary | Rapid Review | Open Access Journal

Received December 14, 2018, accepted February 18, 2019, date of publication February 25, 2019, date of current version March 12, 2019.

Digital Object Identifier 10.1109/ACCESS.2019.2901517

Graphene Enhanced Leaky Mode Resonance in Tilted Fiber Bragg Grating: A New Opportunity for Highly Sensitive Fiber Optic Sensor

ZHIHONG LI[1,2], ZHUYING YU[1], YUBING SHEN[1], XIUKAI RUAN[1,2], AND YUXING DAI[1,2]

[1]College of Mathematics, Physics and Electronic Information Engineering, Wenzhou University, Wenzhou 325035, China
[2]National-Local Joint Engineering Laboratory of Electrical Digital Design Technology, Wenzhou University, Wenzhou 325035, China

Corresponding author: Zhihong Li (zhihonghnu@hotmail.com)

This work was supported by the National Natural Science Foundation of China under Grant 61671329.

This paper has supplementary downloadable material available at http://ieeexplore.ieee.org, provided by the author.

ABSTRACT Tilted fiber Bragg grating (TFBG) presents many unique spectral characteristics for sensing. The widespread approaches to date are based on the cut-off mode resonance and surface plasmon resonance (SPR), whereas the leaky mode resonance is ignored in the literature. Herein, we theoretically demonstrate that the s-polarized (or TE/HE) leaky mode resonance (and the guided mode resonance) can be efficiently enhanced (and suppressed) by integrating graphene on the TFBG for a highly sensitive sensor. In contrast, the p-polarized (or TM/EH) mode (both leaky mode and guided counterpart) presents slight variation. The enhancement principle is discussed based on the variation in the mode characteristics induced by the graphene. The results show that the graphene enhanced leaky mode resonance presents ultra-sensitive intensity response but insensitive wavelength response to the extremely small analyte perturbation. The sensitivities are achieved up to 14108dB/RIU and 5232.6dB/RIU for the first two leaky modes in gaseous media respectively, which are 121 and 13 times higher than that of bare TFBG. This novel sensing platform provides a promising technique that can compete with the widespread SPR approach in fiber optic sensing fields, which opens up new opportunities for industrial, environmental, and biochemical sensing applications.

INDEX TERMS Tilted fiber Bragg grating, graphene, leaky mode resonance, refractive index sensing.

I. INTRODUCTION

The tilted fiber Bragg grating (TFBG) is a special fiber grating that has the refractive index perturbation plane tilted with the fiber axis [1]. Due to this tilted structure, the TFBG presents many unique spectral characteristics, like the Bragg resonance and dense comb-like resonance resulted from the simultaneous mode coupling from forward-propagating core guided mode to backward-propagating core guided mode and hundreds of cladding modes respectively [2]. The dense comb-like resonance of the TFBG provides a promising sensing platform to measure surrounding refractive index (SRI), which can be used to determine analytes' properties, such as purity, concentration, quality, etc [3]. Meanwhile, the Bragg resonance shows insensitive response to the SRI and temperature perturbation and therefore, it can be used as reference band to remove the temperature interference. In recent years, the TFBG has been widely utilized in industrial, environment and bio/chemical sensing applications [3]. The widespread approaches to date are based on the cut-off mode resonance and surface plasmon resonance (SPR) [4]. The cut-off mode corresponds to the boundary between leaky mode and cladding guided mode. When the SRI increases, more cladding guided modes become leaky and hence the boundary (or cut-off wavelength) shifts towards longer wavelength. As a result, the cut-off mode shows sensitive response to the SRI perturbation varying in a large range [5]. The SPR can be excited by phase-matching cladding guided mode of the TFBG coated with nano-meter metal film [6]. The SPR is highly polarization-dependent and can only be excited by p-polarized (or TM-polarized) cladding modes. At the inner surface of metal film, the incident cladding guided mode coupled from the core guided mode is internally reflected but can also be phase-matched to a SPR mode (corresponding to the

The associate editor coordinating the review of this manuscript and approving it for publication was Weidong Zhou.

SPR excitation) at the outer surface of the metal film. When this phase-matched coupling occurs, the reflected cladding guided mode loses power and the SPR induces an intense field localization at outer metal boundary [3]. This coupling also gives rise to the amplitude decrease in the corresponding cladding mode resonance, which means that the occurrence of SPR weakens the cladding mode resonance. To achieve strong SPR, the metal layer must be thin enough to let some light tunnel across [7]. Due to strong evanescent field of the SPR mode in external media, the SPR is greatly affected by the SRI variation and becomes a promising platform for sensing [3], [4].

Generally, the sensing performance corresponding to both the cut-off mode and SPR is evaluated by the wavelength interrogation method, i.e., by tracking the resonance wavelength shift with the SRI perturbation. The resonance wavelength is dependent on the phase-matching condition (PMC). In this case, the highest sensitivity S_{sri} is numerically less than or approximately equal to grating period Λ of the TFBG (i.e., $S_{sri} \leq \Lambda$ in magnitude) [7]. Therefore, the wavelength interrogation method could not be appropriate in some cases where the analytes experience a very small SRI perturbation (such as $10^{-4}RIU$ or even smaller in which RIU represents refractive index unit). This is because that the small external refractive index variation induces extremely small resonance wavelength shift that cannot be accurately tracked by the optical spectrum analyzer (OSA) [8]. In contrast, the intensity interrogation method by measuring the resonance intensity that varies with the SRI perturbation presents a higher sensitivity [8]–[11]. By this approach, it has been demonstrated that the cut-off mode, the last cladding guided mode, SPR mode, and 'apolarized' mode show sensitive response to the SRI perturbation [8]–[12]. For instance, the differential spectrum between p-polarized and s-polarized resonances of the last cladding guided mode provides a self-referenced tool to achieve ultra-high sensitivity and small limit of detection (LOD) [8]. To measure accurately the resonance intensity varying with the external SRI perturbation in actual applications, the ideal method is to filter the transmission spectrum of the TFBG by adding an bandpass filter with the center wavelength equal to the resonance wavelength. However, the analytesâĂŹ perturbation can induce the variation in both resonance amplitude and resonance wavelength. Therefore, filtering the transmission spectrum at the resonance wavelength that varies with the analytes' perturbation in real time becomes a challenge in real applications.

In this work, we demonstrate that the s-polarized leaky mode resonance can be greatly enhanced by integrating graphene on the TFBG and ultra-high sensitivity is achieved in gaseous media with extremely small SRI perturbation. Since the first discovery in 2004, the graphene has attracted extensive attentions due to its exceptional properties, such as large surface-to-volume ratio, high carrier mobility, and excellent tunable photoelectric property [13], [14]. Various graphene integrated optical fiber devices have been reported for sensing applications [15]. Most of those methods need to break the fiber structure to enhance the evanescent field in the graphene and external analyte media [16]–[21]. Recently, the graphene integrated TFBG has been reported for enhancing sensitivity using conventional intensity interrogation for humidity or low SRI sensing [22], [23]. However, the weak leaky mode resonance has been ignored in all previous researches and remains uninvestigated in the literature. Here we report that the graphene enhanced s-polarized leaky mode resonance presents ultra-sensitive intensity response but insensitive wavelength response to the external SRI perturbation. Apparently, this insensitive wavelength response benefits greatly the intensity measurement by bandpass filtering the transmitted spectrum of the TFBG at the leaky mode resonance wavelength in real applications. The enhanced mechanism is explored by the influence of the graphene on the mode characteristics. The results show that the leaky mode resonance presents higher sensitivity than that using classical TFBG and widespread SPR approach. As such, the graphene enhanced leaky mode resonance provides a novel promising sensing platform, which can compete with the widespread SPR method.

The rest of this paper is organized as follows. In section II, the experimental consideration, simulation model, and coupled mode theory of the graphene integrated TFBG sensing platform are presented. The sensing performance of the graphene integrated TFBG sensor is investigated in section III, where the enhancement mechanism, transmission evolution, and comparison with the widespread SPR approach are also discussed. Finally, the conclusion is presented in section IV.

II. EXPERIMENTAL CONSIDERATION AND THEORETICAL MODEL

A. DESIGN OF SENSING SYSTEM

The typical sensing system in experiment is illustrated in Fig. 1(a). The incident light launched from broadband source transmits through the polarizer followed by a polarization controller, and then a linearly polarized light (i.e., p-polarized or s-polarized) or an un-polarized light is introduced into the TFBG. After interacting with the external analyte, the transmission spectrum is recorded by the OSA and the data are analyzed by the computer (PC) to assess the sensing performance of the TFBG sensor. Here the intensity interrogation method by measuring the variation in the resonance intensity (ΔI_{res}) with the SRI perturbation is used to evaluate the sensing performance. In this case, when the SRI changes from n_{sri} to $n_{sri} + \Delta n_{sri}$, where Δn_{sri} is the SRI perturbation, the resonance amplitude changes accordingly. The external analyte is assumed to be gaseous media in simulation. Here the air environment with initial refractive index equal to 1.0 is considered [24]. The maximum SRI perturbation is $\Delta n_{sri} = 5 \times 10^{-4}$ which corresponds to an extremely small analyte perturbation. In general, the optical fiber grating based sensors become insensitive in this low SRI environment since the analytes' refractive index is much

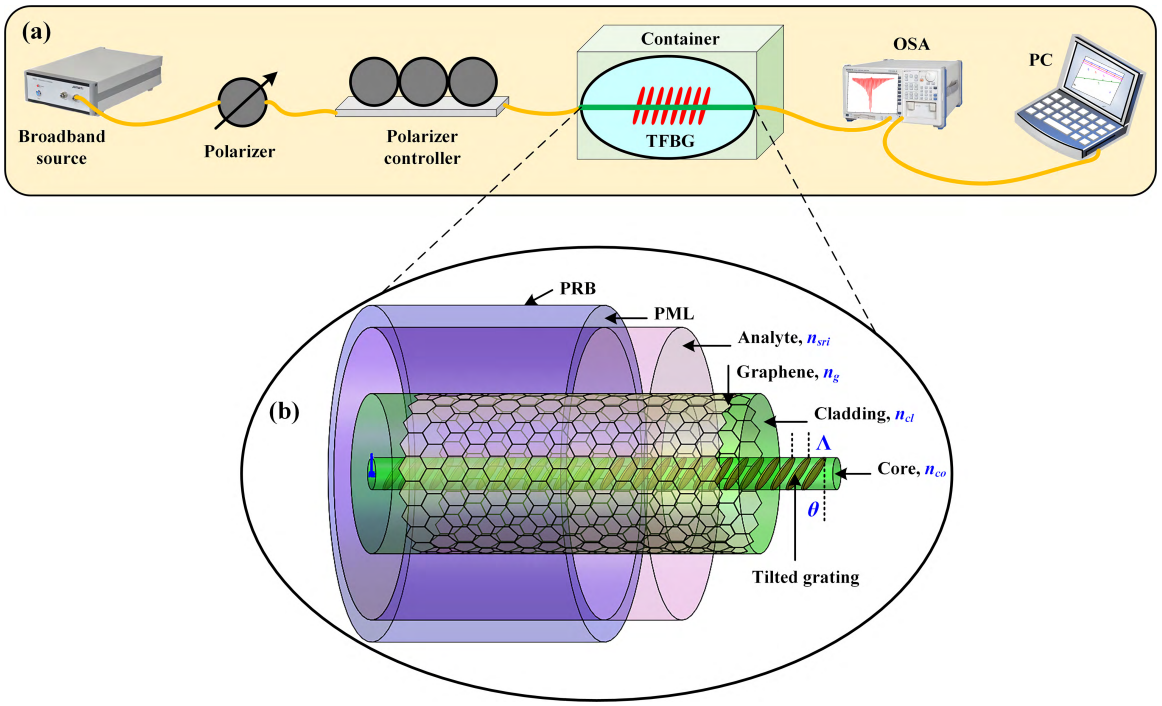

FIGURE 1. (a) Schematic of the TFBG sensing system in experiment. (b) Theoretical diagram structure of the graphene integrated TFBG. PML: perfect matching layer; PRB: perfect reflecting boundary.

smaller than that of fiber cladding. In this insensitive SRI region we investigate and demonstrate the highly sensitive performance of the graphene enhanced leaky mode resonance of the TFBG.

Under the consideration above, the sensitivity that is the most crucial parameter to characterize a sensor is defined as the change in the resonance intensity for an unit change in the SRI of the gaseous media, which is given by:

$$S_{sri} = \left| \frac{\Delta I_{res}}{\Delta n_{sri}} \right| \quad (dB/RIU) \tag{1}$$

wherein the absolute value is taken into account for comparison.

B. SIMULATION THEORY

The TFBG is assumed to be inscribed in commercial single mode fiber (i.e., Corning SMF-28e+) with fiber core radius of $4.1\mu m$ and cladding of $62.5\mu m$. The Sellmeier relation is used to determine the wavelength-dependent dispersion of the fiber cladding, which is given by [25]:

$$n_{cl}(\lambda) = \sqrt{1 + \frac{a_1\lambda^2}{\lambda^2 - \lambda_1^2} + \frac{a_2\lambda^2}{\lambda^2 - \lambda_2^2} + \frac{a_3\lambda^2}{\lambda^2 - \lambda_3^2}} \tag{2}$$

in which λ is the wavelength measured in micrometers. a_i and λ_i are the Sellmeier coefficients and for pure silica glass their values are given by:

$$\begin{aligned} &a_1 = 0.6961663, \quad a_2 = 0.4079426, \quad a_3 = 0.8974794, \\ &\lambda_1 = 0.0684043\mu m, \quad \lambda_2 = 0.1162414\mu m, \quad \lambda_3 = 9.896161\mu m \end{aligned} \tag{3}$$

The refractive index of the fiber core n_{co} is 0.36% higher than that of the cladding according to the products specifications for the Corning SMF-28e+ optical fiber.

Here it is assumed that a five-layer graphene is wrapped on the TFBG to tune sensor performance. Generally, the conductivity σ_g consisting of the interband σ_{inter} and intraband σ_{intra} components of the monolayer graphene can be calculated using the Kubo formula: $\sigma_g = \sigma_{inter}(\omega, T, \Gamma, \mu_c) + \sigma_{intra}(\omega, T, \Gamma, \mu_c)$ in which [16], [18], [26]:

$$\sigma_{intra} = \frac{je^2 k_B T}{\pi\hbar^2(\omega - j2\Gamma)} \left[\frac{\mu_c}{k_B T} + 2\ln\left(e^{-\frac{\mu_c}{k_B T}} + 1\right) \right] \tag{4}$$

$$\sigma_{inter} = \frac{je^2}{4\pi\hbar^2} \ln\left[\frac{2|\mu_c| - (\omega + j2\Gamma)\hbar}{2|\mu_c| + (\omega + j2\Gamma)\hbar} \right] \tag{5}$$

where e is the charge of an electron, $\hbar = h/2\pi$ is the reduced Planck's constant, k_B is the Boltzmann's constant, Γ is the scattering rate, $\omega = 2\pi c/\lambda$ is the radian frequency in which c is the speed of light in vacuum, T is the temperature in Kelvin, and μ_c is chemical potential. The complex refractive index n_g of the graphene can then read as:

$$n_g = \sqrt{1 + j\sigma_g/(\omega\varepsilon_0\Delta)} \tag{6}$$

wherein ε_0 and Δ are the permittivity in vacuum space and graphene sheet thickness, respectively. Consider five-layer graphene, similar electronic structure can be obtained due to the mis-oriented stacking geometry and effective decoupling of adjacent layers [26]. Therefore, the σ_g and n_g of five-layer graphene in this work can also be calculated using the Kubo formula by considering $\sigma_g \to 5\sigma_g$ and $\Delta \to 5\Delta$ [18], [26]. Here typical parameters, i.e., $\Delta = 0.34nm$, $T = 300K$ and

$\Gamma = 0.43meV$, are considered in the following discussion. In this case, the σ_g, and n_g are a function of the chemical potential μ_c that can be dynamically controlled either by chemical doping [27] or by applying a gate voltage [28]. In this work $\mu_c = 0.3eV$ is considered for illustration. Actually, the graphene having $\mu_c <\sim 0.4eV$ or even the pristine graphene without electrically tuning or chemical doping induces very similar influence on the fiber modes' imaginary effective refractive index (ERI, relating to the resonance amplitude) and very similar sensing performance could be obtained [18], [29]. A thorough investigation on the optical properties of the graphene and its influence on the mode characteristics have been detailed in [29]. On this basis, this work focuses on the graphene enhanced leaky mode resonance and the sensing performance improvement.

At the tilted grating region, the mode coupling behavior and transmission spectrum can be described by the coupled mode theory. Here the powerful full-vector complex coupled mode theory [30] combined with an improved piecewise discretization method based finite-difference mode solver [29] is used for the simulation. By this approach, the TFBG sensor is enclosed by the PML and PRB layer and becomes a closed waveguide model, as shown in Fig. 1(b). To facilitate the discussions on the transmission spectrum of the TFBG, the mode coupling equation is simplified as:

$$\begin{aligned}\frac{dA_{11}}{dz} &= -j\kappa_{11}A_{11} - j\sum_{v=0}\sum_{m=1}\kappa_{11,vm}B_{vm}\exp\left(j2\Delta\beta_{vm}z\right),\\ \frac{dB_{11}}{dz} &= j\kappa_{11}B_{11} + j\kappa_{11}A_{11}\exp\left(-j2\Delta\beta_{11}z\right),\\ &\sum_{v=0}\sum_{m=1}\left[\frac{dB_{vm}}{dz} = j\kappa_{vm,11}A_{11}\exp\left(-j2\Delta\beta_{vm}z\right)\right]\end{aligned} \tag{7}$$

in which A_{11}/B_{11} and B_{vm} are the complex amplitudes of forward/backward-propagating core guided mode and the vmth cladding guided mode or leaky mode, respectively, $\Delta\beta_{vm}$ is the tuning factor that is defined in Eq. (8), and $\kappa_{11,vm}$ represents the coupling coefficient which is given in Eq. (9).

$$\Delta\beta_{vm} = Re\left[\frac{1}{2}\left(\beta_{11} + \beta_{vm} - \frac{2\pi}{\Lambda}\right)\right] \tag{8}$$

wherein β is the propagation constant equal to $\beta = 2\pi/\lambda\cdot n_{eff}$ in which n_{eff} is the ERI.

$$\kappa_{11,vm} = \frac{\varepsilon_0\omega n_{co}}{2\hat{K}}\iint\Delta n\left(r,\phi,z\right)\mathbf{e}_{11}\cdot\mathbf{e}_{vm}d\mathbf{s} \tag{9}$$

in which $\mathbf{e}$ is the electric field of a fiber mode, $\hat{K}$ represents the normalized coefficient that is given by $\hat{K} = 1/2\iint(\mathbf{e}\times\mathbf{h})\cdot\hat{z}d\mathbf{s}$ in which $\mathbf{h}$ is the magnetic field, and $\Delta n(r,\phi,z)$ is the tilted refractive index perturbation in fiber core that is determined by Eq. (10). The self-coupling coefficient between the forward- and backward-propagating core guided modes can be also calculated by Eq. (9) under the consideration of $vm = 11$, which corresponds to the core guided mode.

$$\Delta n(r,\phi,z) = \delta n\left[1+\cos\left(\frac{2\pi}{\Lambda}\left(z + r\cos\phi\tan\theta\right)\right)\right] \tag{10}$$

in which δn is the amplitude of the refractive index perturbation and Λ is the axial grating period. In the following analysis, the amplitude of refractive index perturbation, axial grating period and grating length are fixed at 5.0×10^{-4}, $530nm$ and $20mm$ respectively. The calculation and simulation are conducted in MATLAB.

III. RESULTS AND DISCUSSION

A. LEAKY MODE RESONANCE ENHANCED BY GRAPHENE

The PMC of the TFBG is a powerful tool to determine the resonance mode and its resonance wavelength, which is defined as [2]–[4]:

$$\lambda_{res} = 2n_{eff}^{co}\Lambda \tag{11}$$

$$\lambda_{res} = (n_{eff}^{co} + n_{eff,vm}^{cl})\Lambda \tag{12}$$

in which n_{eff}^{co} and $n_{eff,vm}^{cl}$ are the ERIs of the core guided mode and the vmth cladding guided mode or leaky mode (TE/TM$_{0,m}$ and HE/EH$_{v,m}$), respectively. It can be inferred from the PMC that for the TFBG with given period Λ the high-order mode will have its resonance at short wavelength. In our case, the resonance wavelengths of the core guided mode and cut-off mode are approximated to be $\sim1.54\mu m$ and $\sim1.3\mu m$ by assuming $n_{eff}^{co} \approx n_{co}$ and $n_{eff,vm}^{cl} \approx 1.0$, respectively for the weakly guiding single mode fiber. Then the tilted angle of the TFBG is determined to obtain strong comb-like resonance around $1.3\mu m$, which is shown in Fig. S1 in the Supplementary material where only the s-polarized case is considered for illustration. Here the cladding guided modes having $v = 0\sim20$ are taken into account and 10 modes that are closely near the PMC for each v are selected to obtain convergent result [30]. The wavelength step of $0.01nm$ is considered for simulation. As clearly shown in Fig. S1 in the Supplementary material, the comb-like resonance band shifts to shorter wavelength where the higher-order cladding guided modes are excited as the tilted angle increases, which is very similar with the cases reported in [30] and [31]. For a more highly tilted TFBG, two resonance groups could be obtained in gaseous media [10]. For the bare TFBG the leaky mode resonance is much weaker than the cladding guided mode resonance at all tilted angles. After integrating the graphene on the TFBG, however, the leaky mode resonance in air environment is efficiently enhanced whereas the guided counterpart is greatly weakened at $\theta = 24°$.

The more informative properties of the transmission spectra of uncoated and graphene integrated 24° TFBG are reported in Fig. 2 where only the spectrum around the leaky mode resonance is considered to get a clear comparison. The bare TFBG shows strong cladding guided mode resonance in both polarized cases at long wavelength but weakens sharply its amplitude from the cut-off mode at short wavelength

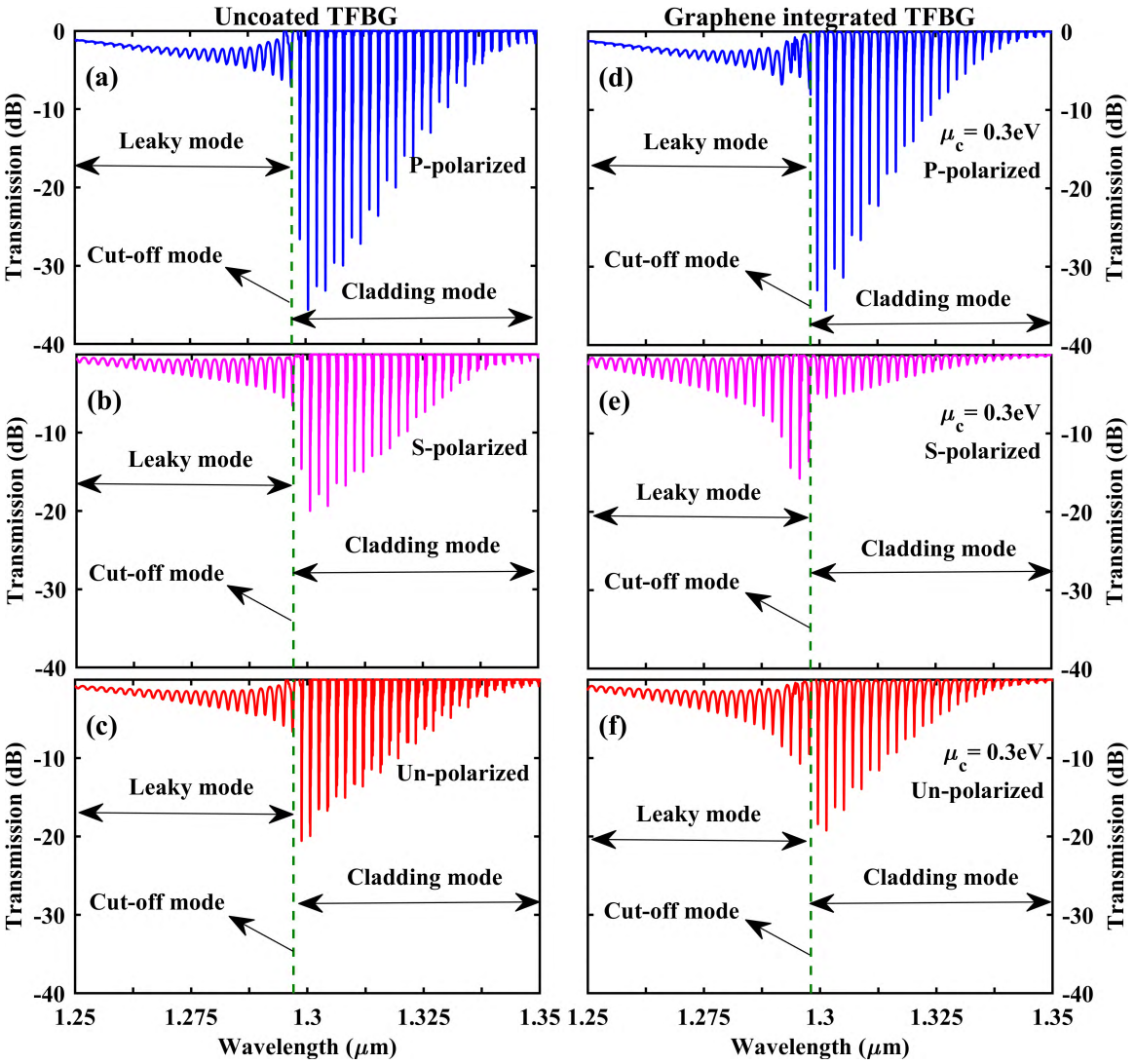

FIGURE 2. Polarized transmission spectra of uncoated TFBG (left) and graphene integrated TFBG (right) in different polarized states at n_{sri} = 1.0. (a) and (d): p-polarized; (b) and (e): s-polarized; (c) and (f): un-polarized.

where the leaky mode resonance occurs. As clearly shown, the leaky mode resonance is so weak that it generally cannot be used for sensing. After integrating the graphene, however, much stronger leaky mode resonance is achieved and meanwhile the cladding guided mode resonance is substantially suppressed in s-polarized case. The amplitude of the leaky mode resonance could even be further improved over 20dB in magnitude when a more exact tilted angle around 24° is considered. In contrast, the p-polarized case presents a slight variation. Also, the leaky mode resonance could not be clearly observed when an un-polarized (or hybrid polarization) incident light consisting of both p- and s-polarized states is considered, as shown in Fig. 2(c). This phenomenon confirms the polarization-dependent property of the graphene enhanced leaky mode resonance, which will be analyzed below. It therefore obviously illustrates from Fig. 2 that the graphene induces much larger influence on the s-polarized mode than the p-polarized case, which is quite the opposite of the widespread phenomenon of SPR that can only be excited by the p-polarized light [6], [7], [10].

B. ENHANCEMENT MECHANISM

To get a deep insight into such an enhanced phenomenon induced by the graphene, the ERI of fiber mode is depicted in Fig. 3. Typically, the fiber mode can be classified into two groups, including guided mode with $n_{sri} < Re(n_{eff}) < n_{co}$ and leaky mode having $Re(n_{eff}) < n_{sri}$, as illustrated in Fig. 3(a). More specifically, the leaky mode consists of two groups, i.e., the guided-like mode (small $Im(n_{eff})$) having the mode field very similar with the guided mode but with a large part outside the fiber structure, and the radiation-like mode (large $Im(n_{eff})$) with an extremely small field content within the fiber region, as shown in Fig. S2 in the Supplementary material where the TE mode is depicted as an illustration.

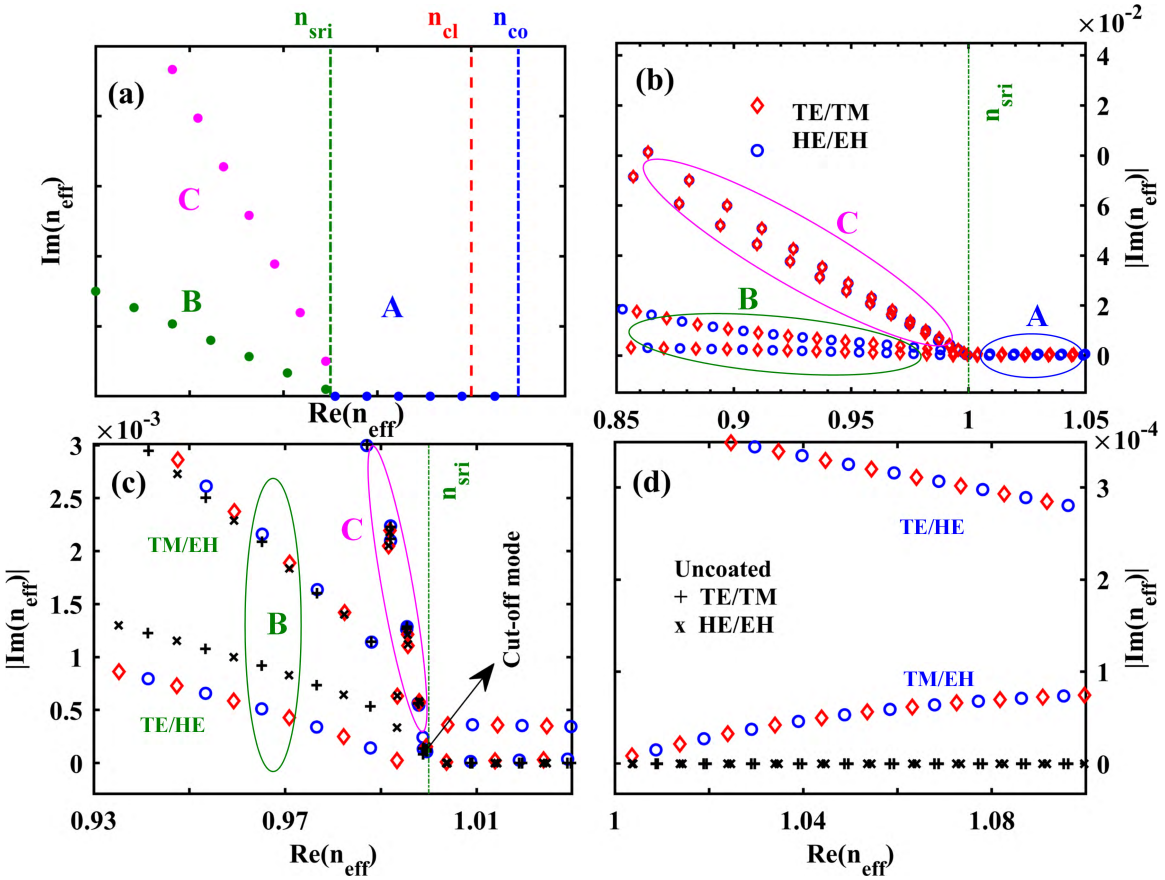

FIGURE 3. (a) Classification of fiber modes. A: guided mode; B: guided-like leaky mode; C: radiation-like leaky mode. (b) The ERI of five-layer graphene integrated TFBG at $\lambda = 1.3\mu m$. (c) and (d) The ERI around n_{sri}.

Apparently, the guided core mode could not couple with the radiation-like leaky mode due to its large $Im(n_{eff})$ and small field content in fiber core. A more specific illustration is reported in Fig. 3(b)∼(d) where the label of TM/EH represents the p-polarized mode and the TE/HE corresponds to the s-polarized counterpart [7]. It is found that a large difference in the $Im(n_{eff})$ between these two polarized modes is obviously observed whereas the opposite trend is achieved for the $Re(n_{eff})$. Particularly, the p-polarized guided-like leaky mode has a larger $Im(n_{eff})$ and the same is true for the s-polarized guided mode. Therefore, stronger leaky mode resonance but combined with a weaker guided mode resonance is obtained for the graphene integrated TFBG in s-polarized state. The p-polarized counterpart presents the exactly opposite phenomenon (also see Fig. 2). In addition, the uncoated case is also depicted for comparison. As clearly illustrated, the graphene induces a smaller $Im(n_{eff})$ for the guided-like TE/HE leaky mode (but larger $Im(n_{eff})$ for the guided TE/HE mode) whereas an extremely small change in the $Re(n_{eff})$ is obtained. As a result, the s-polarized leaky mode (and guided mode) resonance after integrating graphene becomes stronger (and weaker) than that of uncoated case, but only with a slight variation in the resonance wavelength, as illustrated in Fig. 2. It is reasonable to infer that very similar wavelength sensitivity (using the wavelength interrogation method) could be obtained for both uncoated and the graphene integrated TFBG sensors, but a large difference in the intensity sensitivity (evaluated by the intensity interrogation approach) is expected, especially for the leaky mode resonance.

Another important property is about the cut-off mode. In general, the cut-off mode corresponds to the 'interface' between the leaky mode and cladding guided mode [8]. Here we demonstrate that the cut-off mode is the mode having the $Re(n_{eff})$ extremely close to but very slightly smaller than n_{sri} and also having the $Im(n_{eff})$ relatively larger than that of the adjacent cladding guided mode, as shown in Fig. 3(c). Therefore, the cut-off mode can be approximately but reasonably grouped into the leaky mode (guided-like component).

It is noteworthy to mention that the leaky mode resonance was not observed in recent experimental reports [22], [23], which seems to be different from our case. This can be explained in terms of the polarization-dependent condition of the leaky mode resonance. As shown in Fig. 3, the graphene induces a significant variation in the s-polarized mode whereas very small change is obtained for the p-polarized case. When only s-polarized incident light is considered, the leaky mode resonance can be efficiently enhanced and clearly recognized (see Fig. 2). However, the leaky mode resonance will be 'weakened' for an un-polarized light

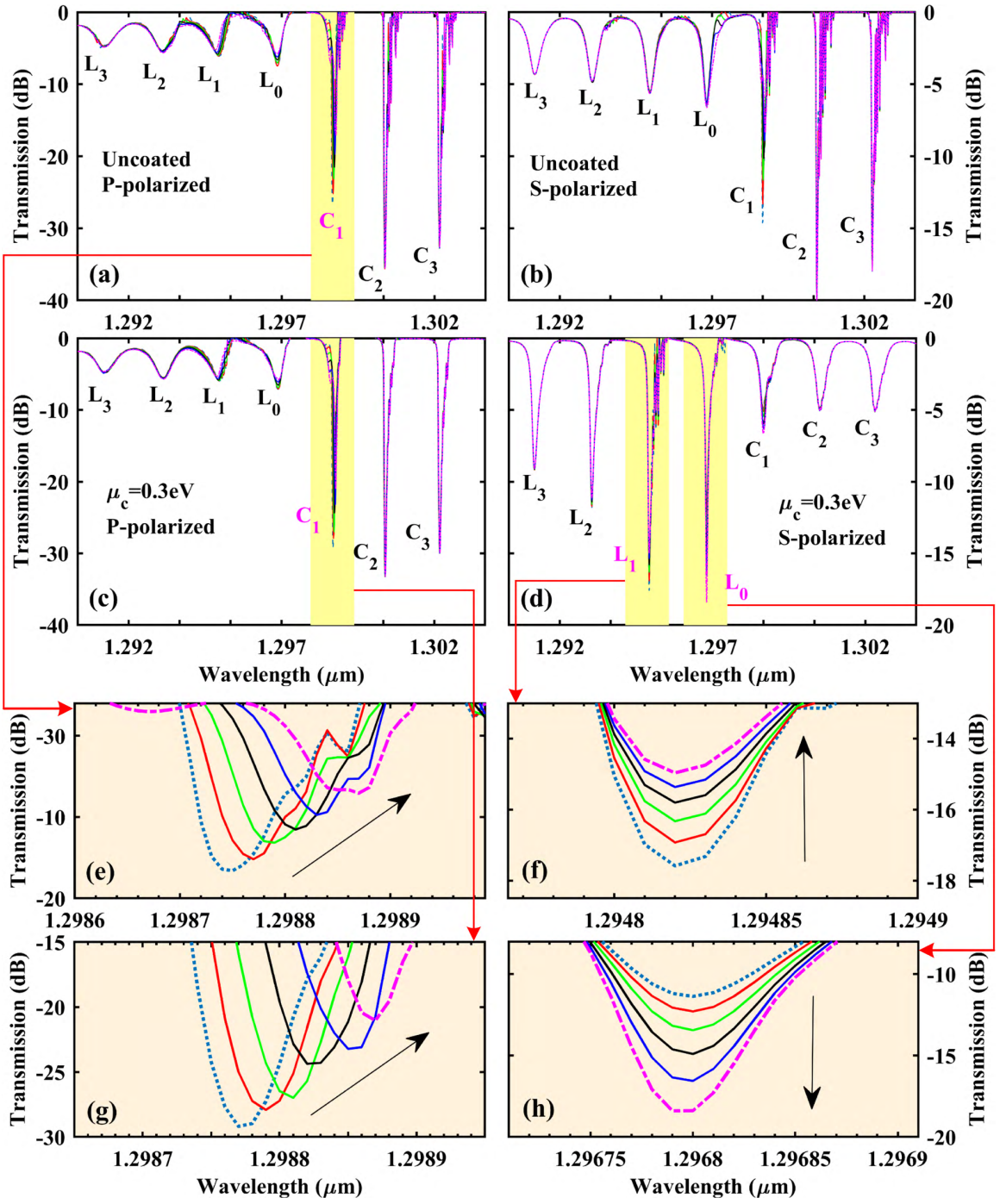

FIGURE 4. Spectrum evolution around the cut-off mode resonance of uncoated and graphene integrated TFBG with the SRI changing from 1.0 to 1.0005 (with a step of 1.0×10^{-4}): (a) and (c) p-polarized case; (b) and (d) s-polarized case; (e) and (g) zoom-in plot of C_1 resonance; (f) zoom-in plot of L_1 resonance; (h) zoom-in plot of L_0 resonance. The dotted line and point-horizontal line in the zoom-in plots represent $n_{sri} = 1.0$ and 1.0005, respectively. The notation L_i/C_i represents the leaky/guided mode.

consisting of both p- and s-polarized states due to the spectrum superposition of these two polarized cases. This corresponds to the situation in Ref. [23] (Ref. [22] only consider the p-polarized light), which is also demonstrated here in Fig. 2(c). As a result, this weak leaky mode resonance could not be clearly recognized in un-polarized state, which is quite similar with the SPR that can only be excited in p-polarized state. In addition, the strong leaky mode resonance also depends on appropriate grating parameters, like a large tilted angle (a weakly tilted TFBG was inscribed in [22] and [23]), as also verified in Fig. S1 in the Supplementary material.

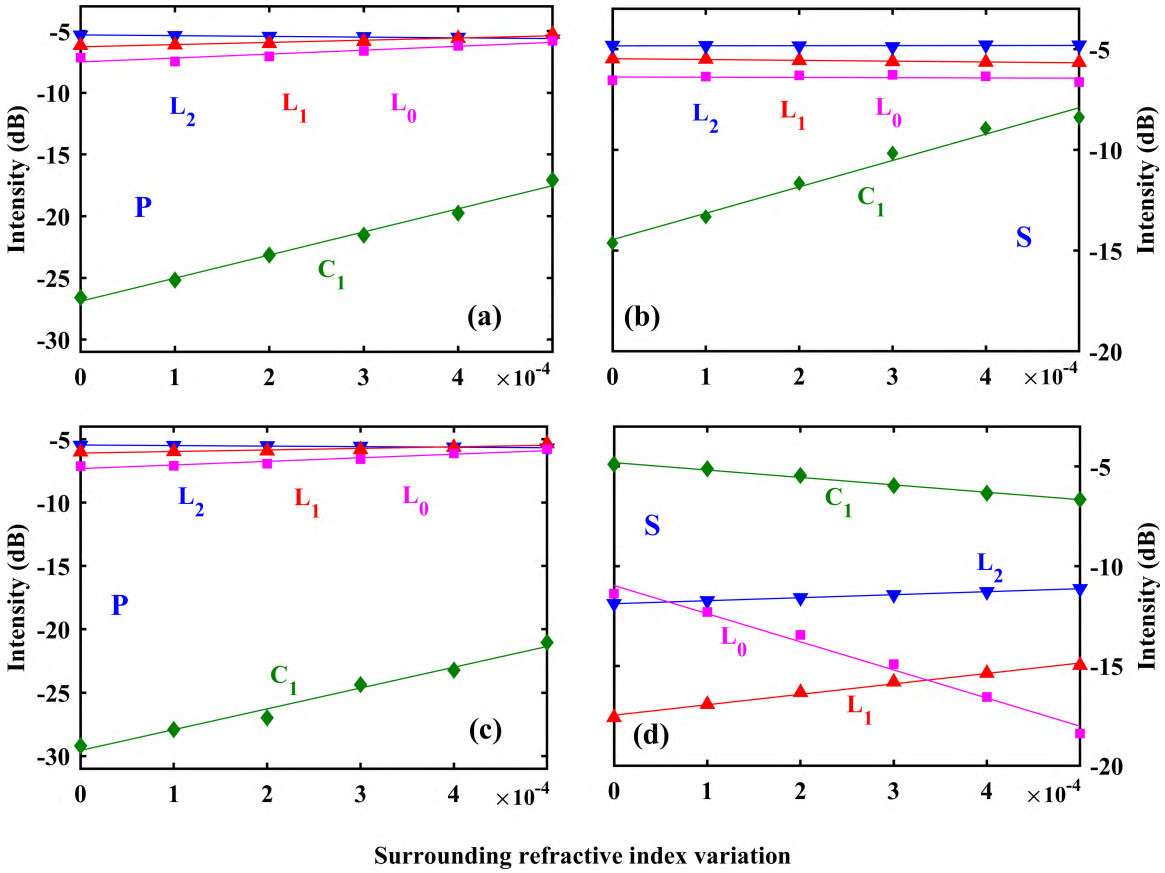

FIGURE 5. Intensity evolution of uncoated (up) and graphene integrated (bottom) TFBG with the SRI perturbation: (a) and (c) p-polarized case; (b) and (d) s-polarized case.

C. TRANSMISSION SPECTRUM EVOLUTION

The spectrum evolution in both polarized states as a function of SRI is depicted in Fig. 4. Here only these resonances around the cut-off mode band labeled as L_0 are considered. For both uncoated and graphene integrated TFBG sensors, all these resonances vary monotonically with SRI but greatly differ in the amplitude and changing trend. Due to the large resonance amplitude, the last guided mode resonance C_1 in both p- and s-polarized cases presents the largest variation (both wavelength and amplitude) for uncoated TFBG. In contrast, all the weak leaky mode resonances show extremely small change and are generally ignored. After integrating the graphene, the p-polarized resonance C_1 appears decrease in the amplitude combined with a red-shift in the wavelength, which is similar with the uncoated case. In contrast, the graphene induces a very different variation trend for the s-polarized case which is detailed by considering L_0 and L_1 leaky mode resonances (see Fig. 4(f) and Fig. 4(h). As clearly observed, the strong leaky mode resonance L_1 decreases its amplitude progressively but keeps the wavelength unchanged during the variation in SRI, whereas the resonance L_0 increases its strength monotonically. This obviously illustrates that the resonance wavelength of the leaky mode is insensitive to the SRI perturbation, which benefits greatly the intensity measurement by bandpass filtering the transmitted spectrum at the resonance wavelength in real applications.

It should be mentioned that the C_2 and C_3 guided mode resonances in all cases almost remain unchanged. In addition, very small variation is obtained for the L_3 and subsequent leaky mode resonances due to relatively small resonance amplitude (the detailed spectrum evolution is omitted here). This evidently indicates that these modes having the ERI ($Re(n_{eff})$) close to n_{sri} present the most sensitive response to the SRI perturbation. On this basis, only the $L_0 \sim L_2$ and C_1 resonances are taken into account to evaluate the sensing performance of the TFBG sensor.

D. SENSING PERFORMANCE

The intensity evolution with the SRI perturbation having the maximum of 5.0×10^{-4} is detailed in Fig. 5. The very small wavelength shift in all cases induced by the extremely small SRI perturbation is not considered since it is too small to be effectively tracked by the OSA. In this case the intensity interrogation method is utilized to assess the sensitivity of the TFBG sensor. Obviously, the p-polarized resonance of the graphene integrated TFBG shows a very similar variation trend with both p- and s-polarized cases of

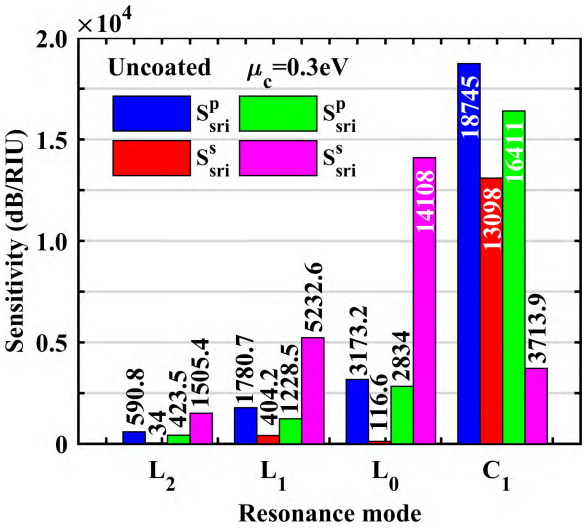

FIGURE 6. Sensing performance of uncoated and graphene integrated TFBG.

uncoated TFBG. This is because that the graphene induces a relatively small influence on the TM/EH mode as discussed above (see Fig. 3). In this situation, the last guided mode C_1 with the strongest resonance among these four bands shows the most sensitive response to the SRI perturbation. In contrast, the graphene integrated TFBG in s-polarized state differs greatly in the intensity evolution as compared with the p-polarized counterpart. In this case, the L_0 leaky mode resonance has the largest variation and becomes the most sensitive band. Also, the L_1 and L_2 with enhanced resonance experience a larger change in the resonance amplitude than that of uncoated case. In addition, the most sensitive C_1 in other cases decreases greatly its intensity response and becomes 'insensitive' to the SRI perturbation, due to the weak resonance suppressed by the graphene (see Fig. 4).

The sensing performance of uncoated and graphene integrated TFBG sensor is reported in Fig. 6 where the sensitivity is evaluated in absolute value for comparison. Considering the leaky mode resonance, one of the most important signature is that the s-polarized leaky mode having an enhanced resonance becomes the most sensitive mode and exhibits the highest sensitivity in each mode group ($L_0 \sim L_2$), as compared with the p-polarized counterpart and p-/s-polarized cases of uncoated TFBG. Here the sensitivity up to 14108dB/RIU and 5232.6dB/RIU for the s-polarized L_0 and L_1 resonances are achieved respectively in gaseous media with an extremely small SRI perturbation, which is improved 121 and 13 times respectively as compared with the uncoated counterpart. As regarding to the guided mode case, the C_1 resonance of uncoated TFBG in both polarized states shows the highest sensitivity (due to a large resonance amplitude). This sensitivity decreases after integrating graphene on TFBG, especially for the s-polarized case (since the graphene significantly weakens its resonance strength as shown in Fig. 2). Though the guided mode C_1 of uncoated TFBG exhibits high sensitivity, both its resonance amplitude and wavelength vary with the SRI perturbation (see Fig. 4). In contrast, the leaky mode almost maintains a constant wavelength, which facilitates the intensity measurement in real situation. On this basis, the graphene enhanced leaky mode resonance provides an alternative but promising tool to achieve highly sensitive gas detection.

E. DISCUSSION

Such novel sensing platform offers a simple structure and higher sensitivity over the widespread SPR approach [10], and interferometric method [16] for gas detection. Generally, the SPR can only be effectively excited at metal film with a certain thickness ($\sim$50 *nm* in liquid environment and $\sim$20 *nm* in gaseous environment) [7], [24]. In our case, the leaky mode resonance is enhanced by decreasing its $Im(n_{eff})$ after integrating graphene (see Fig. 3). Since the graphene is a monomolecular layer 2D material, the number of layers can be easily controlled. This means that this novel sensing platform can be easily fabricated since the key process is to integrate graphene on the fiber cladding of the TFBG, which has been realized recently in [23]. Also, the graphene oxide that has various oxygen groups, such as carbonyl and hydroxyl groups with good biocompatibility, provides an alternative material for selectively biosensing [32]–[36]. For example, the reduced graphene oxide coated fiber Bragg grating has been reported for NO_2 gas detection in [35]. However, the fiber Bragg grating must be etched to enhance the evanescent field of a fiber mode in the external environment. In our case here, the graphene enhanced leaky mode resonance in TFBG without etching process can be used for sensitive NO_2 gas sensing. Since the leaky mode has a larger field outside fiber cladding (i.e., within external environment) than that of cladding and core guided modes, a more sensitive response to the variation of NO_2 gas can be obtained and the sensor becomes more simple and robust.

In addition, the sensitivity can also be evaluated by the approach of differential amplitude (or relative intensity change) to improve the LOD [8], [9]. The intensity variation in L_0 and L_1 differs in the changing trend, i.e., the L_0 decreases with the SRI perturbation but the L_1 increases (or the difference between p- and s-polarized cases), as shown in Fig. 4, which provides a self-referenced tool to measure even smaller SRI perturbation. Since the graphene integrated on the fiber cladding has no effect on the core guided mode confined within fiber core, the Bragg resonance can be used to remove the cross sensitivity resulted from external perturbation, such as optical power fluctuation and temperature. Furthermore, the tunable chemical potential μ_c should also be considered in real applications. For the graphene coated on the TFBG here, the μ_c can be electrically controlled by applying a gate voltage on both ends of this sensing platform, similarly in [26]. According to the aforementioned PMC condition, the leaky mode resonance with ultrahigh sensitivity can also be enhanced in other applications, like the liquid environment having refractive index

around 1.33 corresponding to the general biosensing environment, which opens up new and interesting opportunities for highly sensitive fiber optic sensors.

IV. CONCLUSION

In conclusion, the graphene enhanced s-polarized (or TE/HE) leaky mode resonance in TFBG is demonstrated for gas detection. The integration of graphene layer decreases (and increases) the $Im(n_{eff})$ of the TE/HE leaky mode (and guided mode), which gives rise to a great enhancement (and suppression) of the leaky mode resonance (and guided mode). Meanwhile, the p-polarized (or TM/EH) mode shows a small change both in the ERI and resonance amplitude. The enhanced leaky mode resonance presents ultra-sensitive intensity response but insensitive wavelength response to the SRI perturbation. The results show that the sensitivity of the leaky mode is higher than that of widespread SPR and interferometric approach in gaseous media. This novel sensing platform shows good potential in industrial, environmental, and biochemical sensing applications.

ACKNOWLEDGMENT

The author would like to thank Z. Li Prof. J. Albert at Carleton University for his helpful discussions on mode coupling behavior of highly tilted TFBGs.

REFERENCES

[1] K. S. Lee and T. Erdogan, "Fiber mode coupling in transmissive and reflective tilted fiber gratings," *Appl. Opt.*, vol. 39, no. 9, pp. 1394–1404, Mar. 2000.
[2] X. Dong, H. Zhang, B. Liu, and Y. Miao, "Tilted fiber Bragg gratings: Principle and sensing applications," *Photon. Sensors*, vol. 1, no. 1, pp. 6–30, Mar. 2011.
[3] J. Albert, L.-Y. Shao, and C. Caucheteur, "Tilted fiber Bragg grating sensors," *Laser Photon. Rev.*, vol. 7, no. 1, pp. 83–108, Jan. 2013.
[4] T. Guo, F. Liu, B.-O. Guan, and J. Albert, "Tilted fiber grating mechanical and biochemical sensors," *Opt. Laser Technol.*, vol. 78, pp. 19–33, Apr. 2016.
[5] B. Jiang, K. Zhou, C. Wang, Y. Zhao, J. Zhao, and L. Zhang, "Temperature-calibrated high-precision refractometer using a tilted fiber Bragg grating," *Opt. Express*, vol. 25, no. 21, pp. 25910–25918, Oct. 2017.
[6] Y. Y. Shevchenko and J. Albert, "Plasmon resonances in gold-coated tilted fiber Bragg gratings," *Opt. Lett.*, vol. 32, no. 3, pp. 211–213, Feb. 2007.
[7] C. Caucheteur, V. Voisin, and J. Albert, "Near-infrared grating-assisted spr optical fiber sensors: Design rules for ultimate refractometric sensitivity," *Opt. Express*, vol. 23, no. 3, pp. 2918–2932, Feb. 2015.
[8] T. Guo, F. Liu, Y. Liu, N.-K. Chen, B.-O. Guan, and J. Albert, "*In-situ* detection of density alteration in non-physiological cells with polarimetric tilted fiber grating sensors," *Biosensors Bioelectron.*, vol. 55, pp. 452–458, May 2014.
[9] T. Guo *et al.*, "Highly sensitive detection of urinary protein variations using tilted fiber grating sensors with plasmonic nanocoatings," *Biosensors Bioelectron.*, vol. 78, pp. 221–228, Apr. 2016.
[10] C. Caucheteur, T. Guo, F. Liu, B. O. Guan, and J. Albert, "Ultrasensitive plasmonic sensing in air using optical fibre spectral combs," *Nature Commun.*, vol. 7, Nov. 2016, Art. no. 13371.
[11] Z. Zhang, T. Guo, and B.-O. Guan, "Reflective fiber-optic refractometer using broadband cladding mode coupling mediated by a tilted fiber Bragg grating and an in-fiber mirror," *J. Lightw. Technol.*, to be published. doi: 10.1109/JLT.2018.2838538.
[12] C. Caucheteur, V. Voisin, and J. Albert, "Polarized spectral combs probe optical fiber surface plasmons," *Opt. Exp.*, vol. 21, no. 3, pp. 3055–3066, Feb. 2013.
[13] K. S. Novoselov *et al.*, "Electric field effect in atomically thin carbon films," *Science*, vol. 306, no. 5696, pp. 666–669, 2004.
[14] A. K. Geim, "Graphene: Status and prospects," *Science*, vol. 324, no. 5934, pp. 1530–1534, Jun. 2009.
[15] Y. Zhao, X.-G. Li, X. Zhou, and Y.-N. Zhang, "Review on the graphene based optical fiber chemical and biological sensors," *Sens. Actuators B, Chem.*, vol. 231, pp. 324–340, Aug. 2016.
[16] M. Huang, C. Yang, B. Sun, Z. Zhang, and L. Zhang, "Ultrasensitive sensing in air based on graphene-coated hollow core fibers," *Opt. Express*, vol. 26, no. 3, pp. 3098–3107, Feb. 2018.
[17] A. K. Mishra, S. K. Mishra, and R. K. Verma, "Graphene and beyond graphene MoS_2: A new window in surface-plasmon-resonance-based fiber optic sensing," *J. Phys. Chem. C*, vol. 120, no. 5, pp. 2893–2900, Feb. 2016.
[18] Y. Xiao *et al.*, "Reduced graphene oxide for fiber-optic toluene gas sensing," *Opt. Express*, vol. 24, no. 25, pp. 28290–28302, Nov. 2016.
[19] Y. Wu *et al.*, "Graphene-based D-shaped fiber multicore mode interferometer for chemical gas sensing," *Opt. Lett.*, vol. 39, no. 20, pp. 6030–6033, Oct. 2014.
[20] S. K. Mishra, S. N. Tripathi, V. Choudhary, and B. D. Gupta, "SPR based fibre optic ammonia gas sensor utilizing nanocomposite film of PMMA/reduced graphene oxide prepared by in situ polymerization," *Sens. Actuators B, Chem.*, vol. 199, pp. 190–200, Aug. 2014.
[21] J. A. Kim *et al.*, "Graphene based fiber optic surface plasmon resonance for bio-chemical sensor applications," *Sens. Actuators B, Chem.*, vol. 187, pp. 426–433, Oct. 2013.
[22] Y. Wang *et al.*, "Fiber optic relative humidity sensor based on the tilted fiber Bragg grating coated with graphene oxide," *Appl. Phys. Lett.*, vol. 109, no. 3, p. 031107, 2016.
[23] B. Jiang *et al.*, "Graphene-coated tilted fiber-Bragg grating for enhanced sensing in low-refractive-index region," *Opt. Lett.*, vol. 40, no. 17, pp. 3994–3997, Sep. 2015.
[24] Á. González-Vila, A. Ioannou, M. Loyez, M. Debliquy, D. Lahem, and C. Caucheteur, "Surface plasmon resonance sensing in gaseous media with optical fiber gratings," *Opt. Lett.*, vol. 43, no. 10, pp. 2308–2311, May 2018.
[25] R. Kashyap, *Fiber Bragg Gratings*, 2nd ed. Boston, MA, USA: Academic, 2009.
[26] Q. Bao *et al.*, "Broadband graphene polarizer," *Nature Photon.*, vol. 5, no. 7, pp. 411–415, 2011.
[27] H. Liu, Y. Liu, and D. Zhu, "Chemical doping of graphene," *J. Mater. Chem.*, vol. 21, no. 10, pp. 3335–3345, 2011.
[28] M. Liu *et al.*, "A graphene-based broadband optical modulator," *Nature*, vol. 474, no. 7349, pp. 64–67, May 2011.
[29] Z. Li, Z. Yu, B. Yan, X. Ruan, Y. Zhang, and Y. Dai, "Theoretical analysis of tuning property of the graphene integrated excessively tilted fiber grating for sensitivity enhancement," *J. Opt. Soc. Amer. B, Opt. Phys.*, vol. 36, no. 1, pp. 108–118, Jan. 2019.
[30] Y.-C. Lu, W.-P. Huang, and S.-S. Jian, "Full vector complex coupled mode theory for tilted fiber gratings," *Opt. Express*, vol. 18, no. 2, pp. 713–726, Jan. 2010.
[31] X. Chen, J. Xu, X. Zhang, T. Guo, and B.-O. Guan, "Wide range refractive index measurement using a multi-angle tilted fiber Bragg grating," *IEEE Photon. Technol. Lett.*, vol. 29, no. 9, pp. 719–722, May 1, 2017.
[32] B. Jiang *et al.*, "Label-free glucose biosensor based on enzymatic graphene oxide-functionalized tilted fiber grating," *Sens. Actuators B, Chem*, vol. 254, pp. 1033–1039, Jan. 2018.
[33] C. Liu *et al.*, "Graphene oxide functionalized long period fiber grating for highly sensitive hemoglobin detection," *Sens. Actuators B, Chem.*, vol. 261, pp. 91–96, May 2018.
[34] K. P. W. Dissanayake, W. Wu, H. Nguyen, T. Sun, and K. T. V. Grattan, "Graphene-oxide-coated long-period grating-based fiber optic sensor for relative humidity and external refractive index," *J. Lightw. Technol.*, vol. 36, no. 4, pp. 1145–1151, Feb. 15, 2018.
[35] S. Sridevi, K. S. Vasu, N. Bhat, S. Asokan, and A. K. Sood, "Ultra sensitive NO_2 gas detection using the reduced graphene oxide coated etched fiber Bragg gratings," *Sens. Actuators B, Chem.*, vol. 223, pp. 481–486, Feb. 2016.
[36] S. Sridevi, K. S. Vasu, N. Jayaraman, S. Asokan, and A. K. Sood, "Optical bio-sensing devices based on etched fiber Bragg gratings coated with carbon nanotubes and graphene oxide along with a specific dendrimer," *Sens. Actuators B, Chem.*, vol. 195, pp. 150–155, May 2014.

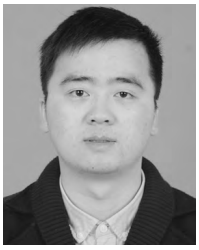

ZHIHONG LI received the Ph.D. degree in optics from Hunan University, Changsha, China, in 2016. He is currently a Lecturer with the College of Mathematics, Physics and Electronic Information Engineering, and also a Researcher with the National-Local Joint Engineering Laboratory of Electrical Digital Design Technology, Wenzhou University, China. His research interests include fiber grating-based sensors and micro-nano photonic devices.

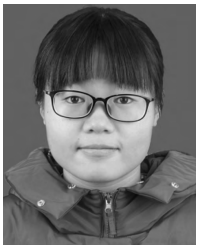

ZHUYING YU is currently pursuing the B.S. degree in telecommunication engineering with Wenzhou University, Wenzhou, China. Her research interest includes design and optimization of fiber grating-based bio-chemical sensors.

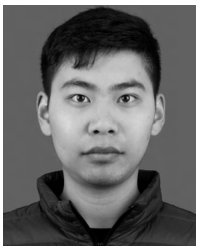

YUBING SHEN is currently pursuing the B.S. degree in telecommunication engineering with Wenzhou University, Wenzhou, China. His research interest includes design and optimization of fiber grating-based bio-chemical sensors.

XIUKAI RUAN received the B.S. degree in automation engineering from the Zhejiang University of Technology, China, in 2001, and the M.S. degree in circuits and systems and Ph.D. degree in signal and information processing from the Nanjing University of Posts and Telecommunications, China, in 2006 and 2011, respectively. He is currently an Associate Professor with the College of Mathematics, Physics and Electronic Information Engineering, and also as the Chief Engineer and the Vice Director of the National-Local Joint Engineering Laboratory for Digitalize Electrical Design Technology, Wenzhou University. His research interests include fiber and radio over fiber communication technology, optical fiber sensors, and information processing counter measure of optical transmission injury.

YUXING DAI received the Ph.D. degree in control theory and control engineering from Central South University, Changsha, China, in 2003. He is currently a National Second-Level Professor with the College of Mathematics, Physics and Electronic Information Engineering, and the Director of the National-Local Joint Engineering Laboratory for Digitalize Electrical Design Technology, Wenzhou University. His research interests include design and fabrication of digital systems, informatization of electrical equipment, and automation control.